

Evaluation of JERS-1 SAR Images From a Coastal Wind Retrieval Point of View

著者	川村 宏
journal or publication title	IEEE transactions on geoscience and remote sensing
volume	42
number	3
page range	491-500
year	2004
URL	http://hdl.handle.net/10097/34955

Evaluation of JERS-1 SAR Images From a Coastal Wind Retrieval Point of View

Teruhisa Shimada, Hiroshi Kawamura, Masanobu Shimada, *Member, IEEE*, Isao Watabe, and Sin-Iti Iwasaki

Abstract—Wind retrieval from Japanese Earth Resources Satellite-1 (JERS-1) synthetic aperture radar (SAR) using an L-band model function in coastal regions is evaluated. It is known that JERS-1 SAR has excessive ambiguities. This paper also gives a quantitative evaluation of excessive ambiguities in coastal scenes of JERS-1 SAR. First, focusing on the cases where wind blows from the shore in Sagami Bay, we investigate phenomena of wind speed increase with offshore distance using European Remote sensing Satellite-1 (ERS-1) SAR-derived wind speeds. The relation between wind speed and offshore distance is well formulated, which indicates the transition of the atmospheric boundary layer from land to sea surface. Wind speeds derived from JERS-1 SAR should be overestimated due to the excessive ambiguity. Then, for observation time of each JERS-1 SAR capturing the cases that wind blows from the shore in Sagami Bay, the expected wind speed growth profile is derived from the wind speed growth formula and an *in situ* wind observation of Hiratsuka Experiment Station. We convert the wind-speed profile into the sigma-0 profile by an L-band model function. Finally, the profiles of JERS-1 SAR-observed and the estimated sigma-0 are compared, and the excessive ambiguity is estimated as the difference between them. As a result, the dynamic range of first azimuth ambiguity is as large as that of the wind-relating signal from the ocean surface. Moreover, higher order azimuth ambiguities and range ambiguity also may have a significant impact on near-shore wind retrieval.

Index Terms—Ambiguities, Japanese Earth Resources Satellite-1 (JERS-1) synthetic aperture radar (SAR), L-band model function, synthetic aperture radar (SAR) wind retrieval.

I. INTRODUCTION

A GEOPHYSICAL model function (GMF) empirically and/or theoretically relates the normalized radar cross section (NRCS) of satellite radar sensors [e.g., scatterometer or synthetic aperture radar (SAR)] at the sea surface to the surface wind speed and direction. Usually, the GMF is also a function of the radar frequency and polarization, incidence angle, and the other minor physical parameters of sea surface. Ku- and C-band model functions are well established and validated through series of satellite scatterometer missions,

i.e., for Ku-band, Seasat/Scatterometer (SASS) [1], National Aeronautics and Space Administration (NASA) Scatterometer onboard the Advanced Earth Observing Satellite (ADEOS) [2], QuikSCAT/SeaWinds (http://podaac.jpl.nasa.gov/quikscat/qscat_doc.html), and for C-band, Active Microwave Instruments (AMI) onboard European Remote sensing Satellite 1 and 2 (ERS-1/2) [3]. SAR images can be converted into wind speed maps using GMF and wind direction from other data sources such as scatterometer, *in situ* measurements, and operational/nonoperational meteorological model outputs. Wind directions can sometimes be extracted from linear features of the images themselves. C-band model functions are used for SAR wind retrieval using ERS-1/2 SAR and RADARSAT (e.g., [4] and [5]). An L-band model function is newly developed by Shimada *et al.* [6] using L-band SAR onboard Japanese Earth Resources Satellite-1 (JERS-1). It enables wind speed retrieval from JERS-1 SAR. Resultant estimates of retrieved wind speeds over the open ocean have a root mean square error (RMSE) of 2.09 m/s with a negligible bias against the truth wind speed [6].

The SAR wind retrieval is especially useful in coastal seas, because SAR can capture the complex wind fields such as orographically modified wind. For its wider applications, it is necessary to validate JERS-1 SAR-derived wind speeds in the coastal zone. It has been already proven that wind speeds derived from JERS-1 SAR using the L-band model function have good accuracy in open oceans [6]. On the other hand, it is known that there exist excessive ambiguities in JERS-1 SAR images due to some system operating troubles in the initial mission check period and that these can contaminate signals from ocean [7]. However, little attention has been given to the point, and quantitative evaluations of excessive ambiguities on JERS-1 SAR images are not understood exactly. So, the effects of excessive ambiguities on wind retrieval in coastal zones are also unknown.

Here, one must notice the wording of “excessive ambiguities.” When the data sequence from a radar is sampled, the presence of ambiguities must be considered. Ambiguities are unwanted contributions to the image. They are always present due to pulse repetition from the radar and the resulting aliasing, which are inherent to radar systems. In most SARs under the present circumstances, the azimuth and range ambiguities should not be a contamination source of the signal of interest, by design. However, JERS-1 SAR is an exception. The contribution from ambiguities that originate from bright targets such as land are so significant that they can contaminate the signal of interest. In such cases, ambiguities cannot be neglected. Therefore, we use the term “excessive ambiguities”

Manuscript received December 4, 2002; revised October 15, 2003.

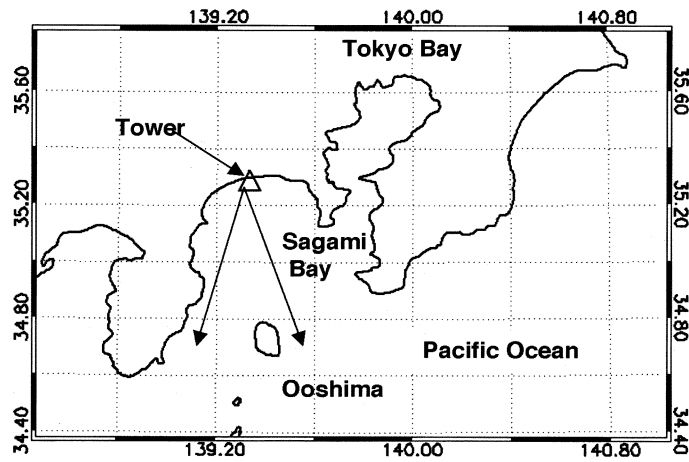
T. Shimada and H. Kawamura are with Center for Atmospheric and Oceanic Studies, Graduate School of Science, Tohoku University, Sendai, 980-8578 Japan (e-mail: shimada@ocean.caos.tohoku.ac.jp; kamu@ocean.caos.tohoku.ac.jp).

M. Shimada is with the Earth Observation Research and application Center, Japan Aerospace Exploration Agency, Tokyo, 104-6023 Japan, (e-mail: shimada@eorc.nasda.go.jp).

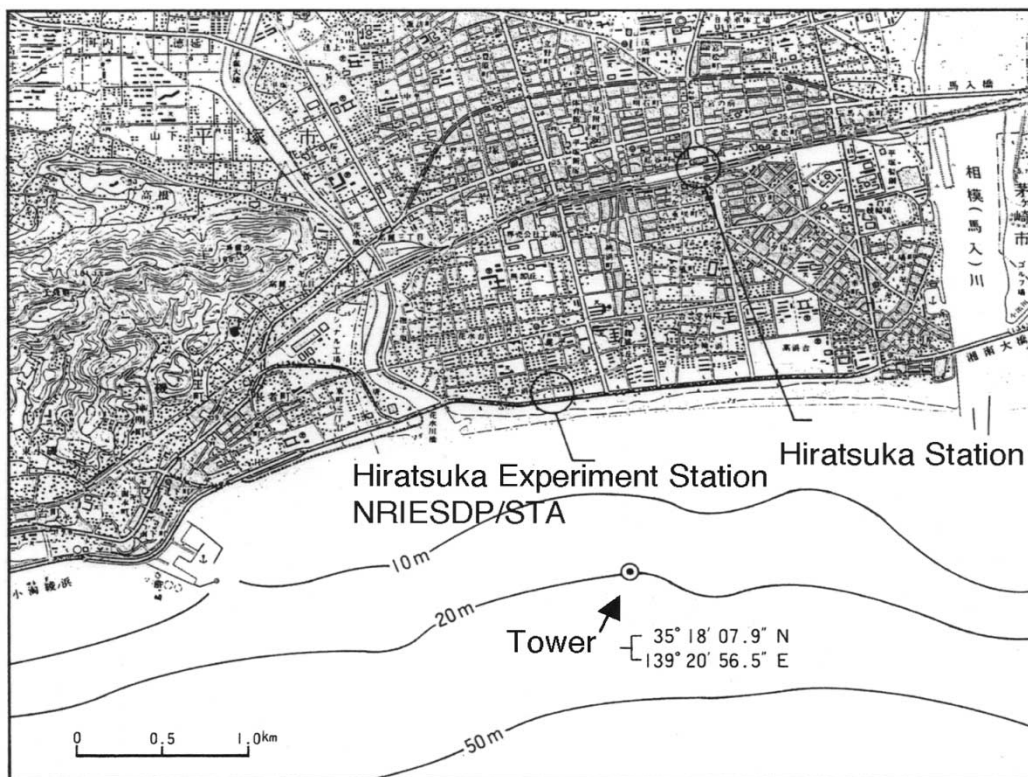
I. Watabe is with Hiratsuka Experiment Station, National Research Institute for Earth Science and Disaster Prevention (NIED), Kanagawa, 254-0813 Japan (e-mail: watabe@bosai.go.jp).

S.-I. Iwasaki is with National Research Institute for Earth Science and Disaster Prevention, Tsukuba, 305-0006 Japan (e-mail: cuh@bosai.go.jp).

Digital Object Identifier 10.1109/TGRS.2003.821268



(a)



(b)

Fig. 1. (a) Geographical locations of the Hiratsuka tower (triangle). In case winds are blowing from north, profiles of JERS-1 SAR sigma-0, ERS-1 SAR NRCS, and wind speeds are obtained along the lines in the area that are indicated between two arrows. (b) The detail map around the Hiratsuka tower.

to refer to the significant ambiguities of JERS-1 SAR in order to differentiate them from ambiguities in an ordinary sense. It is verified in [6] that the ambiguities are not significant in open oceans because the results of wind retrieval are good. Because the intensity of backscattering from sea surface is originally weak compared with that from land, the resulting ambiguities are not significant.

The purpose of this paper is to examine wind retrieval from JERS-1 SAR in coastal seas. It is possible to characterize the results of the present study as evaluation of excessive ambiguities of JERS-1 SAR from a coastal wind retrieval point of view.

Wind speeds derived from ERS-1 SAR and *in situ* wind measurements are used for the validation of JERS-1 SAR-derived wind speeds. The study area is Sagami Bay, where high-quality measurements of winds and waves are made at an observation station. Moreover, the coastline is perpendicular to the azimuth direction. In the following section, data used in the present study are summarized, including a brief review of the L-band model function. The preliminary results are also shown. The method of estimating excessive ambiguities is described in Section III, and Section IV shows the results. Section V is devoted for discussion. Summary and conclusions are given in Section VI.

II. DATA AND METHOD

A. *In Situ* Wind Measurement

Since 1965, sea-surface wind vectors and surface waves have been continuously measured at the Hiratsuka Experiment Station (hereafter, the Hiratsuka tower) operated by the National Research Institute for Earth Science and Disaster Prevention, Japan. The Hiratsuka tower is located 1 km offshore [see Fig. 1(a) and (b)] at a water depth of 20 m. An anemometer is installed on the tower at 19.5 m height above the mean sea surface. Winds and waves are recorded with a sampling interval of 0.3 s. Wind data are recorded hourly as a mean over a period of 10 min. The systems and climatological analyses are summarized in [8] and [9]. The time difference between the *in situ* and SAR observations is less than 30 min. Wind speed at 19.5 m is reduced to 10-m height wind speed by applying a correction factor for neutral stability [10]; in this case, wind speeds are divided by 1.075.

B. JERS-1 SAR and L-Band Model Function

JERS-1 was launched on February 11, 1992. The SAR onboard JERS-1 operated at L-band, horizontal polarization with beam center incidence angle of 39° , and 18-m surface resolution. The swath is 75 km. The SAR data are processed by the Sigma-SAR processor [11]. A total of 110 JERS-1 SAR images at Sagami Bay are used in the present study. (Note: the Sigma-SAR processor uses 70% of the bandwidth, which is centered at the Doppler frequency, mainly for improving the focusing and partially for reducing the azimuth ambiguity.)

Fig. 2(a) and (b) shows schemes of range and azimuth ambiguities in Sagami Bay, respectively. Ambiguities come from outside of the intended imaging target and are folded into the backscattering intensity of the target. Range ambiguities [12] arise from scatterers at either side of 90 km [7] away from the JERS-1 SAR imaging point [Fig. 2(a)]. On the other hand, azimuth ambiguities [12] are due to reflections that are captured by the mainlobe edges or sidelobes of the antenna along-track illumination pattern and repeat image elements in the scene at multiples of 17 km [7] in the along-track direction of the swath. The first-order ambiguity, which nearest from the target, is generally the strongest [Fig. 2(b)]. Their intensities decrease with the distance from the true imaging target [7].

Fig. 3 is an example of JERS-1 SAR image of Sagami Bay. We can see the first-order intense azimuth ambiguity in the center part of the scene. The excessive azimuth ambiguities originated from bright targets such as cities are often recognized in the coastal scenes of JERS-1 SAR.

An L-band model function is developed in [6] using 2288 scenes of JERS-1 SAR. A unique aspect of the analysis is that many coincident and collocated wind vectors observed by ADEOS/NSCAT and buoys were compared with JERS-1 SAR NRCS measurements in open oceans. The problem of the system noise peculiar to JERS-1 SAR is solved. The coefficients of the GMF were derived from the dataset. Some studies have proposed simple relationships between wind vectors and L-band NRCS using the satellite-borne, shuttle-based, and airborne L-band systems [13]–[17]. However, their relationships were not completed for full ranges of wind speed and wind

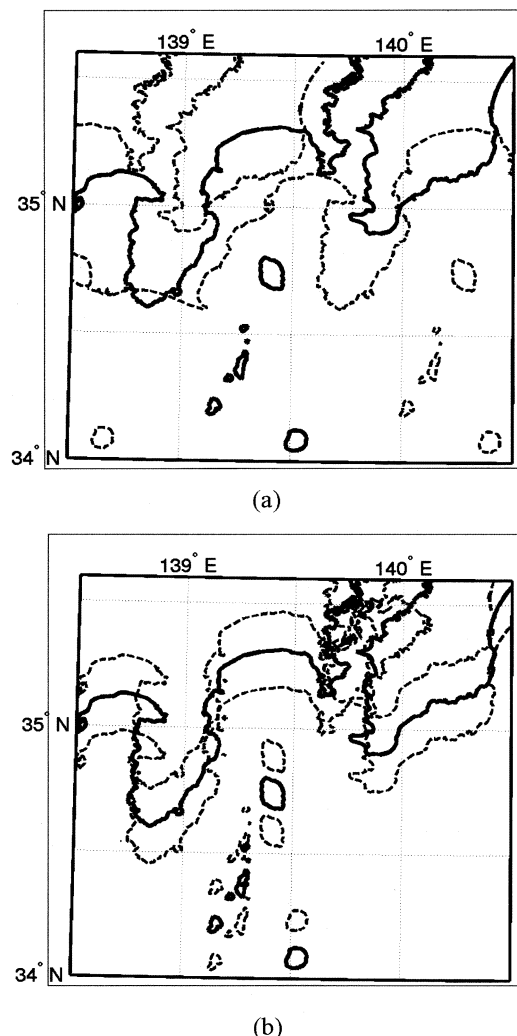


Fig. 2. Schematic locations of (a) range and (b) the first azimuth ambiguity folded from the land around Sagami Bay.

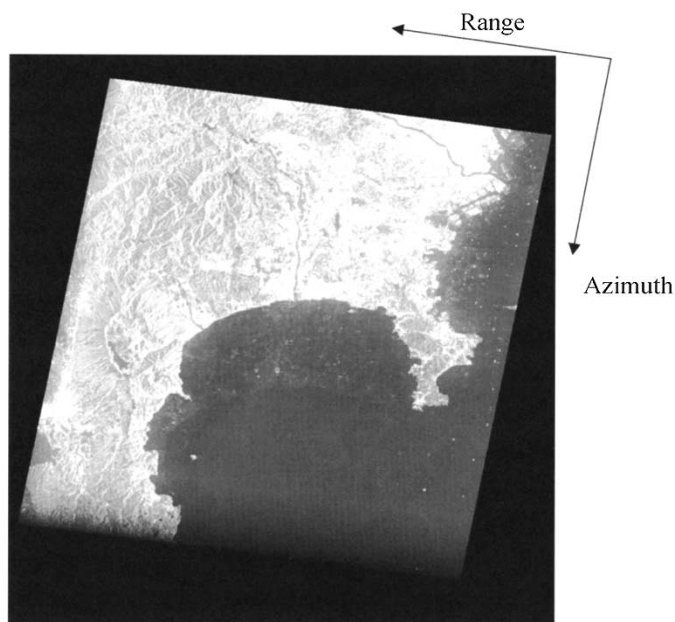


Fig. 3. Example of JERS-1 SAR images of Sagami Bay on April 22, 1992.

direction through examination using statistically significant numbers of measurements. In fact, the large NRCS dataset observed by the JERS-1 SAR is a unique and comprehensive data source of L-band radar backscatter from sea surface.

Main conclusions derived in [6] are as follows.

- 1) L-band NRCS depends on both wind speed and direction. For higher wind speeds, it represents a larger upwind/downwind asymmetry than Ku- and C-band NRCSs. Because of the narrow SAR swath and the system noise of JERS-1 SAR in range direction, they could not examine incidence angle dependence.
- 2) The L-band model function is formulated as the third cosine harmonics of wind direction in order to represent a large upwind/downwind asymmetry. Difference between the wind-speed dependences for upwind and downwind is quite large when the wind speed exceeds 10 m/s. Therefore, conventional second-order harmonics formulas cannot express this deformed wind-direction dependence. In other words, it cannot express the positions of the minimums at 90° and 270° and the large upwind/downwind asymmetry at the same time. The functional form of this L-band model function is

$$\sigma_{\text{lin}}^0 = a_0(U) + a_1(U) \cos \phi + a_2(U) \cos 2\phi + a_3(U) \cos 3\phi \quad (1)$$

for the incidence angle of 37° to 42° and wind speeds 0–20 m/s. U , ϕ , and $a_i/(i = 0, 1, 2, 3)$ represent wind speed, relative wind direction, and model coefficients, respectively. This model function can be considered as the representative relationship between L-band NRCS, wind speed, and wind direction for an incidence angle of 40° .

- 3) Comparison of the SAR-derived wind speeds through the L-band GMF and the sea-truth wind speed results in that the RMSE is 2.09 m/s and the bias is negligible. It is concluded that the proposed L-band model function can convert JERS-1 SAR images of the open ocean into the maps of reliable high-spatial resolution wind speed.

Note that, in the analyses hereafter, we use sigma-0 (σ_{lin}^0) as an alternative to NRCS. It is originally defined in [6] as the square of 16-bit image intensity, from which the system noise level is subtracted. The system noise level is estimated scene by scene. The method of estimating the noise is described in [6]. Namely, the sigma-0 is derived by solving the system noise problem peculiar to JERS-1 SAR. It is verified in [6] that the sigma-0 can be treated as a relatively calibrated backscattering intensity from sea surface and that it is suitable for describing ocean signals of JERS-1 SAR.

In order to investigate the JERS-1 SAR characteristics during the analyzed period, we sample sigma-0 values from 110 scenes of JERS-1 SAR at the Hiratsuka tower. Fig. 4 shows a time series of the differences between sigma-0 observed at the Hiratsuka tower and estimated by the L-band model function with *in situ* wind speed and direction. During the term of JERS-1 initial mission check (February–August 1992), the differences of sigma-0 are fluctuating. Since the start of JERS-1 operational mode at the end of September 1992, the differences of sigma-0 are steady and deviate around a constant level (2.2×10^7). The

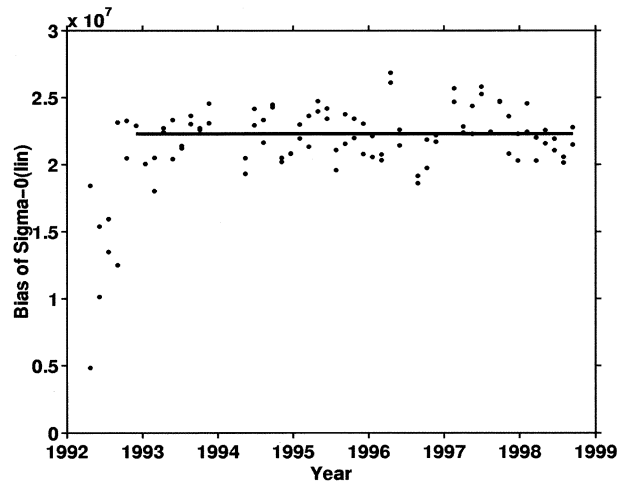


Fig. 4. Difference of the sigma-0 at the Hiratsuka tower observed by JERS-1 SAR and estimated sigma-0 by the L-band model function using the wind speed and direction at the tower. Solid line shows the mean of sigma-0 during the operational mode period of JERS-1 SAR.

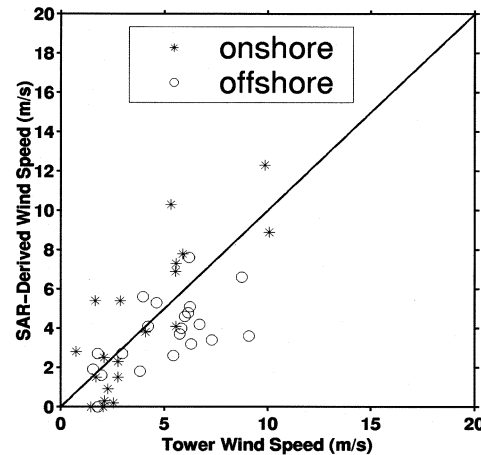


Fig. 5. Comparison of ERS-1 SAR-derived wind speeds with those observed by the Hiratsuka tower 1 km off the coast.

standard deviation is 1.8×10^6 and the relative RMSE is 0.08. In this paper, JERS-1 SAR images obtained during the operational mode period are used.

C. ERS-1 SAR

ERS-1 carried AMI, which could operate as a C-band with vertical polarization SAR. The AMI SAR-mode operates over a fixed range of incidence angles from 20° to 26° , which results in a swath of 100 km. The spatial resolution of the imagery is 30 m. We used 41 scenes from ERS-1 SAR images that view Sagami Bay. The azimuth ambiguity in ERS-1 SAR imagery is not significant. It is verified that the coastal wind retrieval from ERS-1 SAR using C-band scatterometer model functions gives good results (e.g., [18]–[20]).

As a preliminary analysis, we compare ERS-1 SAR-derived wind speeds at the Hiratsuka tower and the *in situ* wind speed measurements at the Hiratsuka tower. Wind speeds are retrieved using the CMOD IFR2 scatterometer wind model [21] and *in situ* wind direction. Fig. 5 shows the results, which are indicated by different symbols for onshore/offshore wind cases. In

the onshore cases, winds are blowing from southwest and southeast, and in the offshore cases the other directions. The resulting RMSE is 2.13 m/s and bias is -0.48 m/s. In conclusion, though retrieved wind are somewhat underestimated, little dependence on the onshore/offshore wind direction is seen, and the wind speeds are generally well retrieved even at near the coast.

III. METHOD

In order to estimate excessive ambiguities and validate JERS-1 SAR-derived wind speeds, we focus on simple cases in which the wind blows from north in Sagami Bay. The range of wind direction observed at the Hiratsuka tower is within 340° to 20° [see Fig. 1(a)]. It is assumed that the wind direction is uniform over the profile line. The method we employed is as follows. First, we derive the profiles of sigma-0 along the assumed wind direction from JERS-1 SAR images. In the same way, NRCS profiles are derived from ERS-1 SAR images. Note that NRCS refers to the absolutely calibrated one. Next, wind speed profiles are derived from the sigma-0 and NRCS profiles using the L- and C-band model functions. The wind speeds derived from JERS-1 SAR should be overestimated due to excessive ambiguities. Then, the wind speed profile derived from ERS-1 SAR is normalized by its mean wind speed. We derive a common feature between them and modeled it by a simple formula. Finally, using this formula and wind speed observed at the Hiratsuka tower, the expected variation of wind speed with offshore distance at the JERS-1 SAR observation time is derived. We convert the wind speed profile into that of sigma-0. The difference between the observed and the estimated sigma-0 profiles are derived as the excessive ambiguities.

The method is concretely described below. Fig. 6(a) shows the variation of wind speed with offshore distance derived from ERS-1 SAR. Each profile is normalized by its mean wind speed. The start point is the location of the Hiratsuka tower. It is clearly shown that wind speed generally increases with the distance from the shore and that all the profiles agree well with each other. Fig. 6(b) shows the mean profile, its standard deviation, and the regression line. The formulation of the regression is defined as

$$\frac{U}{\bar{U}} = a \ln(b(x + c)) \quad (2)$$

where a, b, c are coefficients, x is the offshore distance in kilometers, and \bar{U} is mean wind speed. The values of coefficients are 0.2954, 0.7933, and 5.3476, respectively. The standard deviation is relatively small. It can be concluded that there exists a common feature of wind speed growth with offshore distance in the bay and that the empirically derived profile of wind speed, which is formulated by (2), represents it well.

IV. RESULTS

A. Comparison Between ERS-1 and JERS-1 SAR-Derived Wind Speeds and Tower Wind Speeds

Fig. 7(a)–(d) shows comparisons of SAR-derived wind speeds at the offshore distances of 20, 32, 44, and 55 km, respectively, against the coincident Hiratsuka tower wind speeds for both ERS-1 SAR and JERS-1 SAR. The broken line is a regression line for all the plots. Because the data were not acquired at the

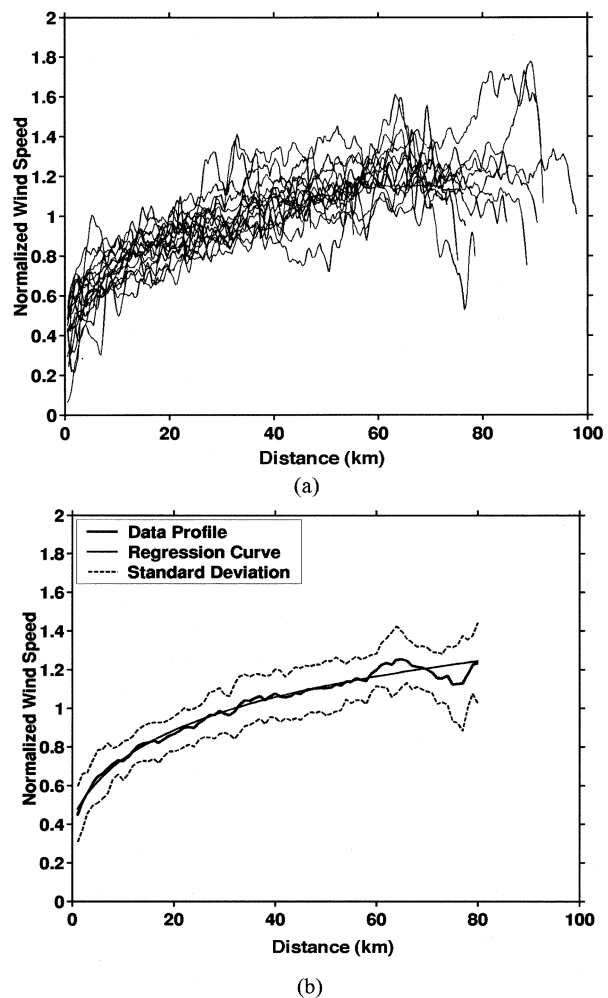


Fig. 6. Variation of wind speed with offshore distance derived from ERS-1 SAR. (a) All profiles of wind speed in northerly wind cases. (b) The mean profile normalized by mean wind speed (thick solid line) and its standard deviations (broken lines). In the figure, the simply formulated variation of wind speed with offshore distance (thin solid line: regression curve) is also shown.

same time for ERS-1 and JERS-1 SAR, we cannot directly compare ERS-1 and JERS-1 SAR-derived wind speeds. So, note the relations between SAR-derived wind speeds and wind speeds observed at the Hiratsuka tower for ERS-1 and JERS-1.

At the distance of 20 km, almost all the wind speeds derived from JERS-1 SAR are larger than 18 m/s, which is due to the excessive ambiguities in the SAR image. At the distance of 32 and 44 km, the JERS-1 SAR-derived wind speeds are much larger than *in situ* wind speeds. In the case of 55-km distance from the shore, both JERS-1 and ERS-1 SAR-derived the wind speeds scatter around the regression line. It is shown that, at the distance of 55 km, the wind speeds derived from ERS-1 SAR and JERS-1 SAR have the same relationship against the Hiratsuka tower wind speeds. The relationship is considered as the growth of wind speed with offshore distance. Wind speeds at the distance of 55 km are about twice as large as those at the tower (located 1 km off shore), which is consistent with the normalized profile of wind speed shown in Fig. 6.

Using (2), wind speeds at the distance of 1 km are estimated from the JERS-1 SAR-derived wind speeds at the distance of 55 km. Fig. 8 shows the comparison between them and the Hiratsuka tower wind speeds. Profiles that do not pass over the

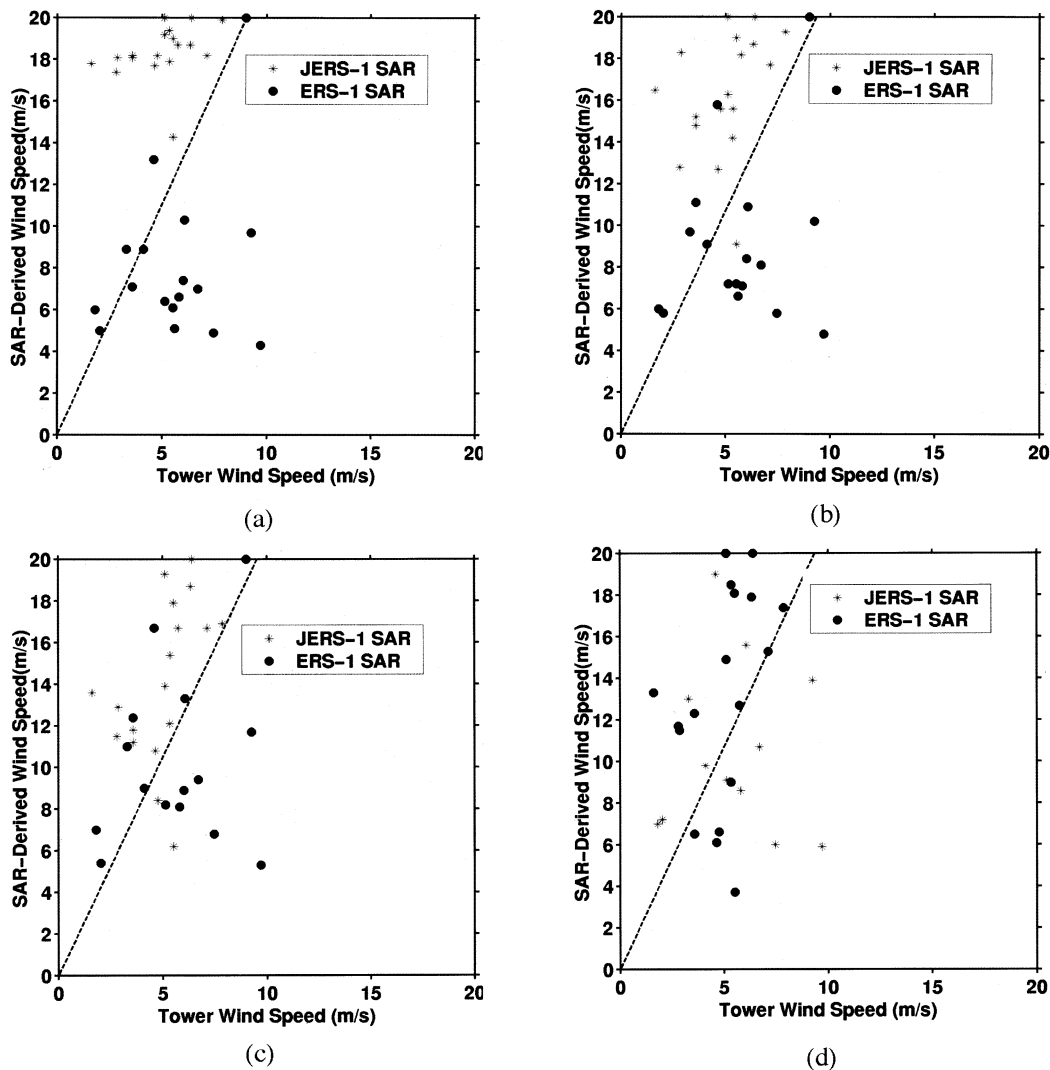


Fig. 7. Comparison of SAR-derived wind speeds at the distance of (a) 20 km, (b) 32 km, (c) 44 km, and (d) 55 km with the Hiratsuka tower wind speeds for JERS-1 SAR and ERS-1 SAR.

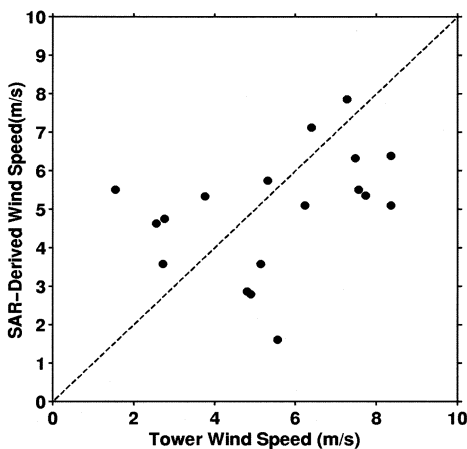


Fig. 8. Comparison of the wind speeds estimated from the JERS-1 SAR images at the distance of 1 km with the tower wind speed. These wind speeds are derived from the wind speed growth formula and JERS-1 SAR-derived wind speeds at the distance of 55 km.

Ooshima are used. The estimated wind speeds agree well with the *in situ* observations; the RMSE is 2.12 m/s, and the bias is 0.51 m/s. This result suggests that the normalized profile of

wind speed represents the growth of wind speed with offshore distance even in the cases of JERS-1 SAR.

B. Estimate of Excessive Ambiguity

On the basis of the above results, the excessive ambiguity is estimated. The solid line in Fig. 9(a) is an example of a profile of JERS-1 SAR sigma-0. The solid line in Fig. 9(b) is the corresponding profile of wind speed by the L-band model function. Using (2) and the JERS-1 SAR-derived wind speed at the distance of 55 km, the expected profile of wind speed is derived [the broken line in Fig. 9(b)]. The corresponding profile of sigma-0, which is derived by the L-band model function, is shown by the broken line in Fig. 9(a). Thus, the difference between SAR-observed and the estimated profiles of sigma-0 is obtained as the excessive ambiguities. These calculations are made for the selected JERS-1 SAR images. In Fig. 9(c), mean profile and the standard deviations of the resulting profiles are shown. It is shown that, within 20 km of offshore distance, the estimated excessive ambiguity is especially high. In the farther distances, excessive ambiguity is little but systematically positive value within 50 km from the coast.

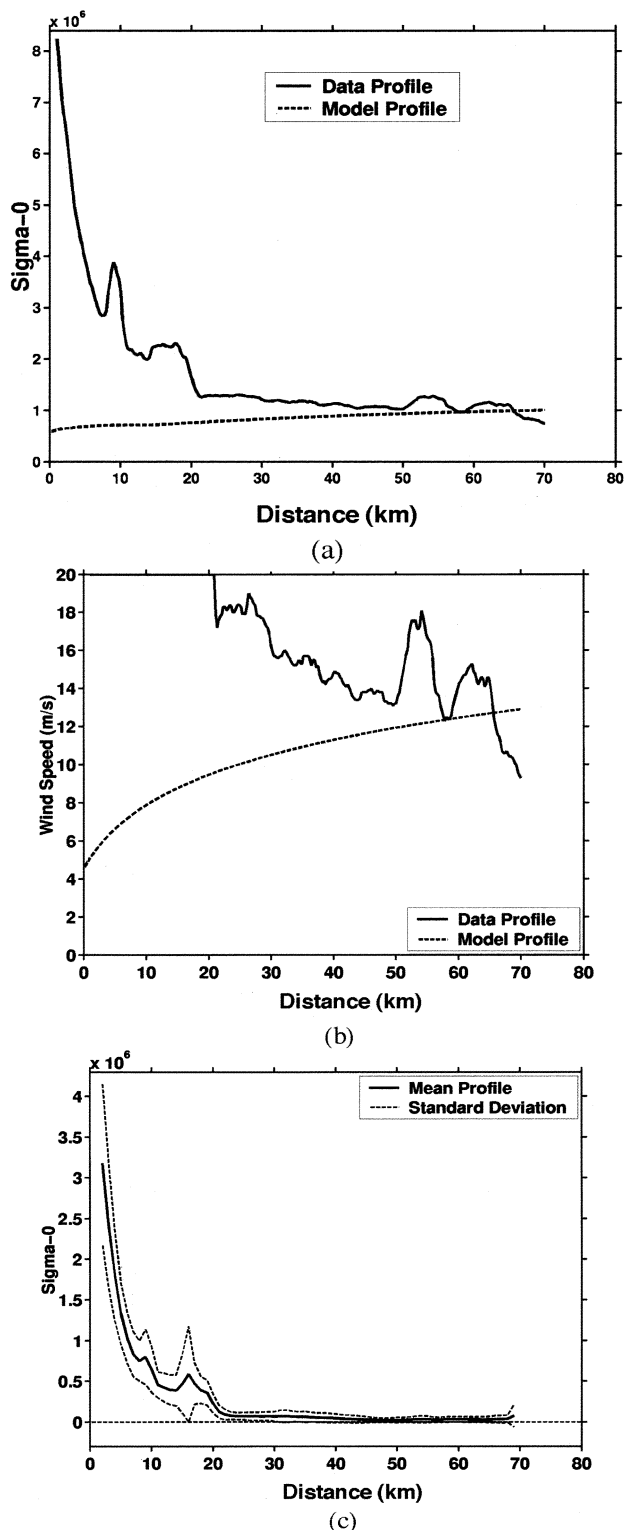


Fig. 9. (a) Profiles of (solid line) the observed sigma-0 and (broken line) the expected sigma-0 (see text). (b) A wind speed profile derived from (solid line) the observed sigma-0 and (broken line) the wind speed profile derived from the wind speed growth formula. (c) Mean profile (solid line) of differences between sigma-0 observed by JERS-1 SAR and sigma-0 estimated by the wind speed growth formula. Two broken lines of a standard deviation are also shown.

V. DISCUSSION

A. Excessive Ambiguities

We estimated the excessive ambiguities as the difference between the observed sigma-0 and the estimated sigma-0 through

the growth of wind speed with offshore distance. It is reasonable to consider the difference of sigma-0 as the excessive ambiguities because the excessive ambiguities are prominent only in the coastal region. The errors due to the wind retrieval and the generalized formula of wind speed growth cause the estimates of excessive ambiguity.

It is reasonable to conclude that excessive ambiguities contaminate the estimated wind speeds from the coastline up to at least 50 km, though the excessive ambiguities become weak with the offshore distance. Within 20 km of distance, excessive ambiguity is especially high. It is considered as the first azimuth ambiguity. It is reported in [7] that the distance at which the first azimuth ambiguity appears is 17 km away.

Wind speeds are overestimated within 50 km from the coast. In the JERS-1 SAR image, it is suggested that not only the first azimuth ambiguity, but also higher order ambiguities and range ambiguity, may have a significant impact on wind retrieval. The relative contributions of the range ambiguity and the higher order azimuth ambiguities cannot be determined.

We consider the ratio of excessive ambiguity to wind signal. The signal-to-ambiguity (SA) ratio is defined by [7] as

$$SA = 10 \log_{10} \left(\frac{I_{\text{ambiguity}}^2 - I_{\text{ocean}}^2}{I_{\text{city}}^2 - I_{\text{ocean}}^2} \right) \quad (3)$$

where $I_{\text{ambiguity}}$, I_{ocean} , and I_{city} indicate the 16-bit image intensity of ambiguity, ocean, and coastal cities, respectively. Here, we simply consider the ratio of the excessive ambiguity to the wind signal.

It is found that sigma-0 corresponding to the wind signal component varies from 0 to 4.0×10^6 for wind speeds of 0–20 m/s according to the L-band model function. On the other hand, the first ambiguity is as large as 2.3×10^6 at the distance of 5 km [Fig. 9(c)]. It can be concluded that the dynamic range of wind signal is as large as that of the first azimuth ambiguity. In other words, the first azimuth ambiguity due to urban reflections has intensities as large as sigma-0 corresponding to high wind speed more than 10 m/s. For example, the ambiguity intensity is 1.0×10^5 at the distance of 40 km even in the third azimuth ambiguity area [Fig. 9(c)]. If the wind speed is 10 m/s, sigma-0 is roughly 1.0×10^6 for all the wind directions according to the L-band model function. In such a case, the error, which is a ratio of ambiguity component to wind signal, can be 10% in estimating sigma-0.

It should be evident that wind speed retrieval from JERS-1 SAR is difficult within 50 km from the coast. When retrieving coastal wind speeds from JERS-1 SAR, we must take into account excessive azimuth and range ambiguities, and we should not use the estimated wind speeds in those areas. However, it is important in the present study that the excessive ambiguities in the ocean of JERS-1 SAR images are quantitatively estimated. These results will be the basis for other ocean applications.

It may be worth mentioning, in passing, that wind signal can be occasionally derived in coastal zones. If the coast is parallel to the azimuth direction, the azimuth ambiguity that arises from coastal areas does not appear in the ocean and does not become a source of noise in estimating sigma-0. Moreover, range ambiguity is not significant compared to azimuth ambiguity. We

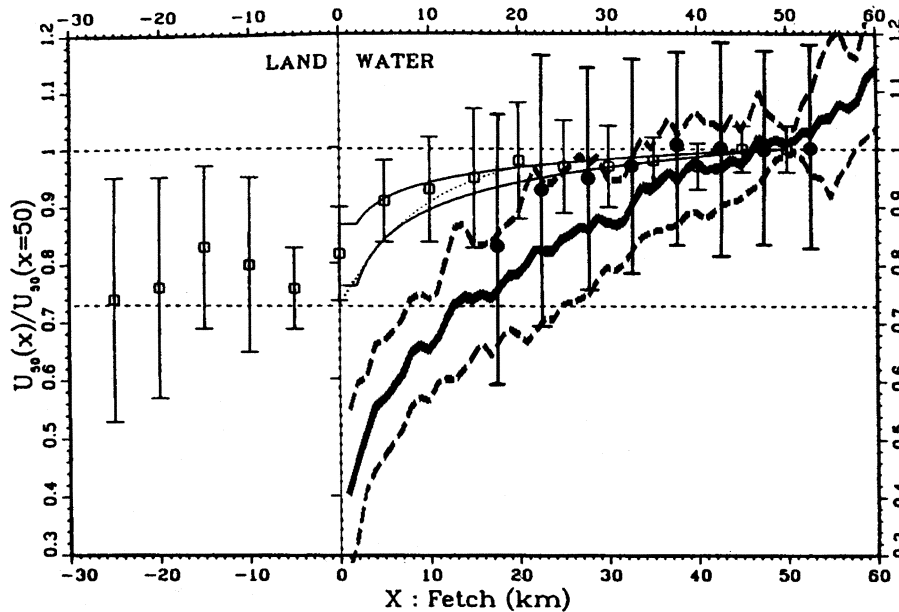


Fig. 10. Comparison of the variation of wind speed derived from the previous studies and the present study. (Black circle) [26]. (Square) Smith/Macpherson field data [24]. (Thin dotted line) Smith/Macpherson empirical fit [24]. (Thin solid line) Taylor/Lee guidelines [23]. Broad solid line and broken lines are the mean and the standard deviations obtained in the present study. Original figure is cited from [25] and [26].

can give an example of the east and west sides of Tohoku area in Japan. If wind speeds are derived in such a case, they will have a relatively low constant bias. If, on the other hand, coastal land is covered by low backscatter and uniform distribution targets, wind signal can be derived even in the presence of the first azimuth ambiguity. The following is a good example. Radar backscatter of JERS-1 SAR and *in situ* wind measurements in the Lake Sinji, Japan are compared in [22]. The lake is surrounded by mountains, and the ambiguities should be folded into the backscattering intensity from the lake. But the relationship between radar backscatter from the lake and wind vectors is consistent with the L-band model function [6].

B. Growth of Wind Speed With Offshore Distance

In this paper, we generalized the growth of wind speed with offshore distance for the northerly wind in the bay (2). It is shown that the wind speed growth profiles normalized by mean wind speed agree well and that ERS SAR wind retrieval is useful for capturing the growth of wind speed with distance from the shore. In this paper, wind direction in the bay is assumed to be uniform as *in situ* observations. But wind direction may not cause significant error of wind speed in the northerly wind cases because the normalized profiles agree well each other.

The growth of wind speed with offshore distance in the bay results from two factors. One is due to the evolution of marine internal atmospheric boundary layers. The aerodynamical roughness over the sea is usually much smaller than that over the land. In coastal seas, the large roughness over the land disappears, and the new internal atmospheric boundary layer starts growing over the sea along the offshore distance. Such relaxation of the internal boundary layer causes the increase of wind speed with distance. The other is due to the effect of upstream

mountainous terrain on the wind. Though the effect of the up-wind terrain decreases with offshore distance, a northerly wind can be influenced by it.

We compare the variation of wind speed with offshore distance derived in the study to those of the previous studies. Several studies investigated the growth of wind speed using the airborne systems, the altimeters, and the scatterometers [23]–[27]. Comparisons between the variations of wind speed in the boundary layers over land/sea in the case of offshore wind are summarized in [26] as shown in Fig. 10. The original figure is adopted from [25]. The relationship derived from ERS-1 SAR in the present study is also shown in Fig. 10. The difference of the heights of wind measurement may not affect the results very much. When the logarithmic wind profile is assumed, the ratio of wind speeds at the two heights is proportional to the root of the drag coefficient [26]. The drag coefficient may change with evolution of wind wave and the atmospheric boundary layer. However, the change of the drag coefficient can be considered to be small and does not affect the results.

The result in this paper is a continuous profile because it is derived from SAR. It has smaller values than those of the other studies within 30-km distance. This suggests that the roughness of upwind city is larger than expected and that coastal wind is influenced by upwind terrain. This may be also due to some effects associated with fetch on radar backscattering.

More studies are required for the growth of wind speed within 100-km scale. It relates the evolution of internal atmospheric boundary layer and the coupling effects of wave and wind under this transition region. For such studies, SAR is a very useful tool.

VI. SUMMARY AND CONCLUSION

In this paper, retrieved wind speeds from JERS-1 SAR in the coastal region are examined, and excessive ambiguities of

JERS-1 SAR are quantitatively estimated. We focus on the cases that wind blows from north in Sagami Bay. We generalized growth of wind speed with offshore distance for northerly wind conditions of the bay using the ERS-1 SAR-derived wind speeds. We estimated the originally expected wind speed profile for each JERS-1 SAR observation time from the generalized wind speed growth formula (2) and *in situ* measurements. The wind speed profile is converted into sigma-0 by the L-band model function. Excessive ambiguities are estimated as the difference between observed and estimated sigma-0.

These observations lead to the following conclusions. The wind speeds estimated from ERS-1 SAR using the C-band model function and from JERS-1 SAR using the L-band model function are consistent at the distance of 55 km away from the coast. It is suggested that not only the first azimuth ambiguity but also higher order azimuth ambiguity and range ambiguity are significant for wind retrieval for JERS-1 SAR, though they are much smaller than the first azimuth ambiguity. The first azimuth ambiguity is large as sigma-0 value of the high wind signals. Wind retrieval from JERS-1 SAR is difficult within 50 km from the coast. It is necessary to bear the excessive ambiguities in mind when using JERS-1 SAR images of coastal regions.

The newly developed L-band model function allows us to estimate JERS-1 SAR excessive ambiguities in coastal seas quantitatively. Unfortunately, it is found that coastal wind retrieval using JERS-1 SAR is difficult. However, this study will be a basis for ocean applications using JERS-1 SAR. Moreover, from the analyses of ERS-1 SAR, SAR can be a useful tool for coastal wind studies.

ACKNOWLEDGMENT

Both JERS-1 and ERS-1 SAR data were provided from National Space Development Agency of Japan. Hiratsuka Experiment Station data were provided by National Research Institute for Earth Science and Disaster Prevention of Japan.

REFERENCES

- [1] F. J. Wentz, S. Peteherych, and L. A. Thomas, "A model function for ocean radar cross sections at 14.6 GHz," *J. Geophys. Res.*, vol. 89, pp. 3689–3704, 1984.
- [2] F. J. Wentz and D. K. Smith, "A model function for the ocean-normalized radar cross section at 14 GHz derived from NSCAT observation," *J. Geophys. Res.*, vol. 86, pp. 11 499–11 514, 1999.
- [3] A. Stoffelen and D. Anderson, "Scatterometer data interpretation: Estimation and validation of the transfer function CMOD4," *J. Geophys. Res.*, vol. 102, pp. 5767–5780, 1997.
- [4] W. Alpers and B. Brümmer, "Atmospheric boundary layer rolls observed by the synthetic aperture radar aboard the ERS-1 satellite," *J. Geophys. Res.*, vol. 99, pp. 12 613–13 621, 1994.
- [5] F. M. Monaldo, D. R. Thompson, R. C. Beal, W. G. Pichel, and P. Clemente-Colòn, "Comparison of SAR-derived wind speed with model predictions and ocean buoy measurements," *IEEE Trans. Geosci. Remote Sensing*, vol. 39, pp. 2587–2600, Dec. 2001.
- [6] T. Shimada, H. Kawamura, and M. Shimada, "An L-band geophysical model function for SAR wind retrieval using JERS-1 SAR," *IEEE Trans. Geosci. Remote Sensing*, vol. 41, pp. 518–531, Mar. 2003.
- [7] M. Shimada, "Calibration and image quality of JERS-1's SAR products," *J. Remote Sens. Soc. Jpn.*, vol. 14, no. 2, pp. 35–46, 1994.
- [8] I. Watabe, Y. Fujinawa, S. Iwata, H. Ishidoya, and I. Isozaki, "Oceanographical and meteorological structure of Sagami Bay (Part 1)," Nat. Res. Inst. Earth Sci. and Disaster Prevention, Tsukuba, Japan, Tech. Note 170, 1996.

- [9] —, "Oceanographical and meteorological structure of Sagami Bay (Part 2)," Nat. Res. Inst. Earth Sci. and Disaster Prevention, Tsukuba, Japan, Tech. Note 177, 1997.
- [10] WMO, "Guide to wave analysis and forecasting," World Meteorol. Org., Geneva, Switzerland, WMO-72, 1998.
- [11] M. Shimada, "Verification processor for SAR calibration and interferometry," *Adv. Space Res.*, vol. 23, no. 8, pp. 1477–1486, 1999.
- [12] F. M. Henderson and A. J. Lewis, *Manual of Remote Sensing*. New York: Wiley, 1998, vol. 2, Principles and Applications of Imaging Radar.
- [13] D. E. Weissman, D. B. King, and T. W. Thompson, "Relationship between hurricane surface wind and L-band radar backscatter from the sea surface," *J. Appl. Meteorol.*, vol. 18, pp. 1023–1034, 1979.
- [14] T. W. Thompson, D. E. Weissman, and F. I. Gonzalez, "SEASAT SAR cross-section modulation by surface winds: GOASEX observations," *Geophys. Res. Lett.*, vol. 8, pp. 159–162, 1981.
- [15] T. W. Gerling, "Structure of the surface wind field from the Seasat SAR," *J. Geophys. Res.*, vol. 91, pp. 2308–2320, 1986.
- [16] W. C. Keller and W. J. Plant, "Cross sections and modulation transfer functions at L and Ku bands measured during the tower ocean wave and radar dependence experiment," *J. Geophys. Res.*, vol. 95, pp. 16 277–16 289, 1990.
- [17] D. G. Long, R. S. Collier, R. Reed, and D. V. Arnold, "Dependence of the normalized radar cross section of water waves on bragg wavelength-wind speed sensitivity," *IEEE Trans. Geosci. Remote Sensing*, vol. 34, pp. 656–666, May 1996.
- [18] T. W. Vachon, O. M. Johannessen, and J. A. Johannessen, "An ERS-1 synthetic aperture radar image of atmospheric lee waves," *J. Geophys. Res.*, vol. 99, pp. 22 483–22 490, 1994.
- [19] S. Lehner, J. Horstmann, W. Koch, and W. Rosenthal, "Mesoscale wind measurement using recalibrated ERS SAR images," *J. Geophys. Res.*, vol. 103, pp. 7847–7856, 1998.
- [20] E. Korsbakken, J. A. Johannessen, and O. M. Johannessen, "Coastal wind field retrievals from ERS synthetic aperture radar images," *J. Geophys. Res.*, vol. 103, pp. 7857–7874, 1998.
- [21] Y. Quifen, B. Chapron, T. Elfouhaily, K. Katsaros, and J. Tournadre, "Observation of tropical cyclones by high-resolution scatterometry," *J. Geophys. Res.*, vol. 103, pp. 7767–7786, 1998.
- [22] K. Ichikawa, T. Kozu, T. Shimoyama, Y. Sakuno, T. Matsunaga, and K. Takayasu, "Feasibility of spaceborne SAR monitoring of coastal lagoon environments," in *Proc. 23rd Int. Symp. Space Technology and Science*, Matsue, Japan, May 26–June 2 2002.
- [23] P. A. Taylor and R. J. Lee, "Simple guide-lines for estimating wind speed variations due to small-scale topographic features," *Climatol. Bull.*, vol. 18, pp. 3–32, 1984.
- [24] P. C. Smith and J. I. MacPherson, "Cross-shore variation of near-surface wind velocity and atmospheric turbulence at the land-sea boundary during CASP," *Atmos. Ocean*, vol. 25, pp. 279–303, 1987.
- [25] F. Dobson, W. Perrie, and B. Toulany, "On the deep-water fetch laws for wind-generated surface gravity waves," *Atmos. Ocean*, vol. 27, pp. 210–236, 1989.
- [26] N. Ebuchi, H. Kawamura, and Y. Toba, "Growth of wind waves with fetch observed by the Geosat Altimeter in the Japan Sea under winter monsoon," *J. Geophys. Res.*, vol. 97, no. C1, pp. 809–819, 1992.
- [27] N. Ebuchi, "Growth of wind waves with fetch in the Sea of Japan under winter monsoon investigated using data from satellite altimeters and scatterometer," *J. Oceanogr.*, vol. 55, pp. 575–584, 1999.

Teruhisa Shimada received the B.S. degree in science from Tohoku University, Sendai, Japan, in 1999, and the M.S. and Ph.D. degrees in geophysics from the Graduate School of Tohoku University, in 2001 and 2004, respectively.

His current research interests are applications of high-resolution satellite images including SAR into air–sea–land interaction studies in coastal zones.

Hiroshi Kawamura received the B.S. degree in science from Tohoku University, Sendai, Japan, in 1978, and the M.S. and Ph.D. degrees in geophysics from the Graduate School of the Tohoku University.

He is currently a Professor with the Center for Atmospheric and Oceanic Studies, Faculty of Science, Tohoku University. His research interests are oceanographic applications of remote sensing methods, i.e., satellite oceanography, and air–sea interaction including small-scale physics at the air–sea interface.

Masanobu Shimada (M'98) received the B.S. and M.S. degrees in aeronautical engineering from Kyoto University, Kyoto, Japan, in 1977 and 1979, and the Ph.D. degree in electrical engineering from the University of Tokyo, Tokyo, Japan, in 1999.

He joined the National Space Development Agency of Japan (NASDA), Tokyo, in 1979. From 1985 to 1995, he developed data processing subsystems for optical and SAR data (MOS-1, SPOT, and JERS-1) at the NASDA Observation Research Center (EORC), Tokyo. He was a Visiting Scientist with the Jet Propulsion Laboratory, Pasadena, CA, in 1990, where he investigated the antenna elevation patterns measurement using in-flight SAR data (SIR-B). After launch of JERS-1 in 1992, he conducted JERS-1 SAR calibration. Since 1995, he has been assigned duties at EORC, where he is in charge of the ALOS/JERS-1 Science project (rainforest mapping projects and SAR interferometry projects). His current research interests are SAR calibration and SAR interferometric applications including polarimetric SAR interferometry (crustal deformation detection, tree height detection, and continental land movement).

Dr. Shimada was awarded the IEEE Interactive Session Prize at IGARSS 2002 for "Correction of the Satellite's Satellite Vector and the Atmospheric Excess Path Delay in the SAR Interferometry: An Application to Surface Deformation Detection." He is Chairman of the CEOS SAR CAL/VAL subgroup. He is also leading an ISPRS Commission I, WG4. He is a member of the Japan Geologic Society and the American Geophysical Union.

Isao Watabe received the bachelor's degree in engineering from Tokyo Denki University, Tokyo, Japan, in 1964.

He joined the Hiratsuka Experiment Station, National Research Institute for Earth Science and Disaster Prevention (NIED), Kanagawa, Japan, in 1967. He has engaged in the development and maintenance of the observation systems of Hiratsuka Experiment Station.

Sin-Iti Iwasaki received the M.S. degree in geophysics from the Graduate School of the University of Tokyo, Tokyo, Japan, in 1980.

From 1984 to 1986, he was a Research Fellow with the Ministry of Education of Japan. In 1986, he moved to the Hiratsuka Branch of National Research Center of Disaster Prevention of Science and Technology Agency, Japan. According to the reorganization of the institute, he moved to the National Research Institute of Earth Science and Disaster Prevention, Tsukuba, Japan as a Senior Researcher in 1992. His main research interest is Tsunami. Since 1996, he has also engaged in study of the sea level rise as a Head of the special project of the institute "Clarification and Prediction of Long-Term Risk Changes in Coastal Disasters."